Acta Oceanol. Sin., 2015, Vol. 34, No. 11, P. 126–135
DOI: 10.1007/s13131-015-0659-y
http://www.hyxb.org.cn
E-mail: hyxbe@263.net

A study on the dynamic tie points ASI algorithm in the Arctic Ocean

HAO Guanghua[1], SU Jie[1]*

[1] Key Laboratory of Physical Oceanography of Ministry of Education, Ocean University of China, Qingdao 266100, China

Received 16 February 2015; accepted 16 April 2015

Abstract

Sea ice concentration is an important parameter for polar sea ice monitoring. Based on 89 GHz AMSR-E (Advanced Microwave Scanning Radiometer for Earth Observing System) data, a gridded high-resolution passive microwave sea ice concentration product can be obtained using the ASI (the Arctic Radiation And Turbulence Interaction Study (ARTIST) Sea Ice) retrieval algorithm. Instead of using fixed-point values, we developed ASI algorithm based on daily changed tie points, called as the dynamic tie point ASI algorithm in this study. Here the tie points are expressed as the brightness temperature polarization difference of open water and 100% sea ice. In 2010, the yearly-averaged tie points of open water and sea ice in Arctic are estimated to be 50.8 K and 7.8 K, respectively. It is confirmed that the sea ice concentrations retrieved by the dynamic tie point ASI algorithm can increase (decrease) the sea ice concentrations in low-value (high-value) areas. This improved the sea ice concentrations by present retrieval algorithm from microwave data to some extent. Comparing with the products using fixed tie points, the sea ice concentrations retrieved from AMSR-E data by using the dynamic tie point ASI algorithm are closer to those obtained from MODIS (Moderate-resolution Imaging Spectroradiometer) data. In 40 selected cloud-free sample regions, 95% of our results have smaller mean differences and 75% of our results have lower root mean square (RMS) differences compare with those by the fixed tie points.

Key words: dynamic tie points ASI algorithm, sea ice concentration, AMSR-E, MODIS

Citation: Hao Guanghua, Su Jie. 2015. A study on the dynamic tie points ASI algorithm in the Arctic Ocean. Acta Oceanologica Sinica, 34(11): 126–135, doi: 10.1007/s13131-015-0659-y

1 Introduction

Arctic sea ice is an indicator and amplifier of polar climate change (Rind et al., 1995; de Vernal et al., 2013). The steady decline of Arctic sea ice has important impacts on both the regional and global climate system through complex feedback processes (Vavrus and Harrison, 2003; Serreze et al., 2003; Liu et al., 2004, Bi et al., 2014). Sea ice concentration, percentage of the area occupied by sea ice, is the most extensively used parameter reflecting the spatial distribution of ice and can be used to calculate the sea ice extent and sea ice area. Therefore, the accuracy of sea ice concentration retrieved from satellite observations is very important.

Microwave remote sensing data of sea ice are an important source of information on sea ice distribution. Compared with other satellite data, microwave remote sensing data are not limited by the polar night and less hampered by clouds. Sea ice concentration derived from passive microwave remote sensing data have a better temporal and spatial continuity.

A series of algorithms have been developed to retrieve the ice concentration from passive microwave data. Among the present most commonly used algorithms, the NASA-Team (NT) algorithm (Cavalieri et al., 1984), the Bootstrap (BT) algorithm (Comiso, 1995) and the dual-polarized ratio algorithm (Zhang et al., 2013) are based on data from the low-frequency bands (19 GHz and 37 GHz), which produce relatively low-resolution ice concentration data (25 km ×25 km). The NASA-Team and Bootstrap sea ice concentration algorithms are the widespread used algorithms (Meier, 2005; Spreen et al., 2008). The NASA-Team2 (NT2) Algorithm (Markus and Cavalieri, 2000) just used the 85 GHz data to mitigate effects due to scattering from snow, but its spatial resolution is still determined by the 19 GHz data. The SEA LION algorithm (Kern, 2001; Kern and Heygster, 2001; Kern et al., 2003) and the ASI (the Arctic Radiation and Turbulence Interaction Study (ARTIST) Sea Ice) algorithm (Kaleschke et al., 2001) all include the SSM/I (Special Sensor Microwave/Imager) 85GHz band data and thus are able to provide ice concentration data with a spatial resolution of 12.5 km (Emery et al., 1994). AMSR-E (advanced microwave scanning radiometer-earth observing system) data based on the ASI algorithm can provide a 6.25 km resolution sea ice concentration product (Spreen et al., 2008). There are currently a variety of sea ice concentration products that correspond to these algorithms (Table 1). But most of the algorithms used by the products are based on low-frequency data, which limit the spatial resolution. Using the 89 GHz frequency data from AMSR-E permits to retrieve the sea ice concentration at 6.25 km grid resolution by ASI algorithm (Spreen et al., 2008).

The sea ice concentration products retrieved from satellite data require sufficient validation and comparison with an independent and reliable source. Higher resolution visible light remote sensing data are important means in comparing with the

Foundation item: The Global Change Research Program of China under contract No. 2015CB953901; the National Natural Science Foundation of China under contract Nos 41330960 and 41276193.
*Corresponding author, E-mail: sujie@ouc.edu.cn

Table 1. The data source, algorithm and the spatial resolution for the main sea ice concentration products

Algorithm	Data source	Spatial resolution
NASA Team (NT)	Nimbus-7 SMMR; DMSP SSM/I-SSMIS	25 km×25 km
NASA Team2 (NT2)	AMSR-E	12.5 km×12.5 km
Bootstrap (BT)	Nimbus-7 SMMR; DMSP SSM/I-SSMIS	25 km×25 km
Bootstrap (BT)	AMSR-E	12.5 km×12.5 km
ASI	AMSR-E	6.25 km×6.25 km
ASI	SSMIS	6.25 km×6.25 km

microwave sea ice concentration products. However, the applications of visible light remote sensing data are restricted because of the impact of clouds and polar night. The data in the visible light frequency with clear sky conditions are selected for comparison. Emery et al. (1994) assessed the SSM/I ice concentrations by using the ice concentration data retrieved from 17 selected AVHRR (Advanced Very High Resolution Radiometer) images using the threshold method. Meier (2005) compared the SSM/I-derived sea ice concentration estimates using four common algorithms (Bootstrap (BT), Cal/Val (CV), NASA Team (NT), and NASA Team 2 (NT2)) using ice concentrations obtained from AVHRR images (17 in winter and 31 in summer) via the threshold method. Cavalieri et al. (2006) used 4 cloud-free ETM+ (Enhanced Thematic Mapper Plus) images to compare with the AMSR-E retrieval sea ice concentration products. They suggested that a way to improve the accuracy of AMSR-E ice concentration estimates was to constantly adjust the algorithm tie points. Han and Lee (2007) selected 68 MODIS (Moderate-resolution Imaging Spectroradiometer) cloud-free images in the Antarctic and used ice classification methods to compare with the AMSR-E sea ice concentrations. Cavalieri et al.(2010) also assessed AMSR-E retrieval products in the Antarctic using 10 MODIS cloud-free images and noted that the ice edge zone was the main source region of errors. Wiebe et al. (2009) used Landsat data to compare with AMSR-E sea ice concentration products and found that using fixed tie points for open water (P_0=47.0 K) and sea ice (P_1=11.7 K) led to most new ice being classified as open water in the ice edge zone. They also found that, compared with the sea ice concentrations retrieved from the SAR (Synthetic Aperture Radar) data, the ASI algorithm underestimates the sea ice concentration at the ice edge and overestimates it in the inner region. Comiso and Kwok (1996) also noted that the microwave algorithm tended to underestimate ice concentrations due to the impact of melt ponds in the summer.

The AMSR-E sea ice dataset, which characterizes sea ice more accurately and with a higher resolution, is an important source of data (Comiso et al., 2003). For ASI algorithm, the polarization difference (vertical minus horizontal) of 89 GHz brightness temperature for open water and 100% sea ice are the two important tie points to retrieve sea ice concentrations. The ASI algorithm which was applied to AMSR-E data (Spreen et al., 2008) mainly used fixed tie points to derive the sea ice concentration all year round. Referring to Eastwood et al. (2011)'s work, this study will develop an improved daily changing tie points ASI algorithm, called as the dynamic tie point ASI algorithm. To demonstrate the advantage of the algorithm, a comparison of the sea ice concentrations retrieved by this improved algorithm with those from the fixed tie points will be given. For further comparison, 40 MODIS images that cover most of the Arctic marginal seas were selected to calculate sea ice concentration with 500-m resolution by tie point algorithm (Steffen and Schweiger, 1991).

In this paper, we will first describe AMSR-E data used to retrieve ice concentrations and the MODIS data used for comparison in Section 2. After that, a developed ASI algorithm is proposed and the impact of clouds on the tie points is presented in Section 3. The subsequent comparison is presented in Section 4. Finally, a brief summary and discussion will be provided.

2 Data set

The ASI algorithm computes sea ice concentration from the polarization difference of 89 GHz brightness temperature (Spreen et al., 2008). Additionally, for application of the weather filters, AMSR-E data from 18.7 GHz, 23.8 GHz and 36.5 GHz vertical channels are required (Spreen et al., 2008). The gridded brightness temperature data in polar stereographic projection, provided by NSIDC (National Snow and Ice Data Center), are used. AMSR-E is a microwave radiometer on board the AQUA satellite platform (the same as MODIS). The 89 GHz band data are at 6.25 km spatial resolution. The brightness temperature data from 18.7 GHz, 23.8 GHz and 36.5 GHz vertical channels are at 12.5 km spatial resolution, which will be linearly interpolated onto the 6.25 km×6.25 km grids to fit the 89 GHz data used for weather filters.

For comparison, the data from MODIS are used. The MODIS sensor provides images of 36 separate spectral bands, ranging in wavelength from 0.4 μm to 14.5 μm. The nadir spatial resolutions are 250 m, 500 m and 1 km, and the swath width is 2 330 km. Here, the MODIS L1B data of Band 1 (0.620–0.670 μm), Band 3 (0.459–0.479 μm) and Band 4 (0.545–0.565 μm) at 500-m spatial resolution were used to obtain sea ice concentrations to assess our results. Meanwhile, in order to compare the sea ice concentration derived from the ASI algorithm based on dynamic tie points (see Section 3) with those based on fixed tie points, we use ASI algorithm sea ice concentration data provided by the University of Bremen within Polarview (Spreen et al., 2008) with the spatial resolution of 6.25 km×6.25 km. The blind zone for the Bremen sea ice concentration is about 88°N, which is different from the NSIDC brightness temperature, which is about 89.24°N.

3 The ASI algorithm based on dynamic tie points

The ASI algorithm was first proposed by Svendsen et al. (1987) and subsequently improved by Kaleschke et al. (2001) for 85 GHz SSM/I data. This algorithm has adopted to use 89 GHz AMSR-E data, as described by Spreen et al., (2008). Unlike other algorithms using near 85 GHz band data, it does not need additional input data (Kern, 2004). The sea ice concentration C is estimated as a function of 89 GHz brightness temperature polarization difference in form of a third-order polynomial, as shown in Eq. (1):

$$C = d_3P^3 + d_2P^2 + d_1P + d_0\,, \tag{1}$$

where P is the polarization difference defined as the brightness temperature difference between 89.0 GHz vertically and hori-

zontally polarized channels, and d_3, d_2, $d_1$and d_0 are the coefficients of the retrieval equation. The coefficients d_3, d_2, d_1 and d_0 are determined by P_0 and P_1, the details of which appear in Spreen et al. (2008)'s Eq. (11). P_0 and P_1 are the polarization difference for open water and 100% sea ice tie points, respectively.

3.1 *The difference between this algorithm and previous algorithms*

The tie points P_0=47 K, P_1=11.7 K used in the ASI algorithm have been chosen based on AMSR-E data (Spreen, 2004; Spreen et al., 2008). Su et al. (2013) obtained the sea ice and open water tie points in the selected fixed regions which were treated as the open water and sea ice to compute the spatial average value all year round. This gave the tie point value a clear physical meaning, but still did not reflect changes of tie points with time. Additionally, the selected sea ice region is near the Canadian archipelago, which is commonly covered by multi-year ice. Therefore, the statistical value obtained by Su et al. (2013) did not take into account the influence of first-year ice. In fact, both Spreen et al. (2008) and Su et al. (2013) showed that P_0 and P_1 have seasonal variations; therefore, dynamic tie points should be more reasonable to be used for sea ice concentration retrieval.

Eastwood et al. (2011) determined the sea ice and open water tie points for the 18 GHz and 37 GHz channels NASA TEAM algorithm products, together with the SSM/I and SMMR (Scanning Multichannel Microware Radiometer) data and produced a dynamic tie points sea ice concentration retrieval algorithm suitable for SSM/I and SMMR data. It is obvious that the choice of tie points depends on the accuracy of the NASA TEAM algorithm products.

The dynamic tie point algorithm on sea ice concentration retrieval proposed here does not need additional ice concentration products.

Firstly, according to the statistical analysis of AMSR-E data during 2003–2006 by Spreen et al. (2008), we chose the floor 40.0 and 7.7 K as the initial values for P_0 and P_1, respectively, for the daily preliminary sea ice concentrations. Secondly, without any weather filters, we computed the new daily P_0 and P_1 averaged within the selected open water and sea ice regions (see Fig. 1). Sea ice concentrations of 0% and greater than 95% according to the daily preliminary sea ice concentrations are selected, shown as the regions outlined with blue and cyan lines, respectively. We use 95% to ensure there are enough ice points to calculate the sea ice tie point. And the daily spatial averages of the P are treated as the open water and sea ice tie points to derive the sea ice concentration again. This step ensures that the influence of clouds on the calculation of open water values is minimized by filtering the spurious ice induced by cloud. Finally, we use the new tie points resulting from the second step to calculate sea ice concentrations and apply the first two weather filters (Gloersen and Cavalieri, 1986; Cavalieri et al., 1995) mentioned in Spreen et al. (2008) to filter out spurious ice. The whole process is shown in Fig. 2. To determine the open water tie point, a ratio of the vertical polarization channel brightness temperatures of 18.7 GHz and 36.5 GHz is introduced as a criterion (Zhang, 2012).

3.2 *The influence of clouds on the calculation of tie points*

The AMSR-E 89 GHz data are sensitive to cloud liquid water, water vapor and cyclones of weather systems, particularly in the open water region. Therefore, the existence of clouds will change the polarization differences of sea water, making the open water tie point value smaller, and lead to more spurious sea ice during the retrieval process. So this spurious response should be removed in the statistics of the open water tie point. Three weather filters are introduced by Spreen et al. (2008), the first two use the gradient ratios $GR(36,18)$ and $GR(23,18)$ with $GR(X,Y)=[TB(X,v)-TB(Y,v)]/[TB(X,v)+TB(Y,v)]$, which can be used to filter the spurious sea ice generated by clouds and water vapor. In the first step of calculation of sea ice concentrations, we did not use the above two filters. By comparing the sea ice concentrations after using the above two filters, we can find which grid has spurious ice due to influence of clouds. Thus the grid points affected by the clouds will not be included in the calculation of the open water tie point by using the second step results, which will minimize the influence of clouds. Figure 3 shows the effect of clouds on the calculation of open water tie point. Before the influence of clouds is filtered, the open water tie point has a relatively small yearly-average value (38.5 K) and larger variation (5.1 K), along with a significant decrease in summer. After the clouds are filtered, the

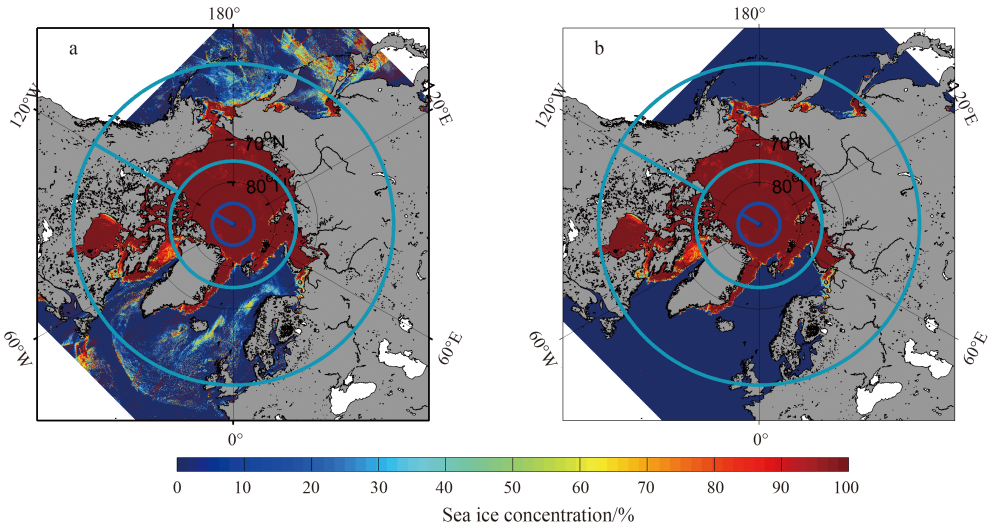

Fig. 1. Regions of the tie point calculation. The sea ice concentrations retrieved in the first step are shown in shading area, the selected regions for calculating sea ice and open water tie points are outlined with dark (within 85°–89.24°N) blue circle and cyan loop (within 53°–75°N), respectively (a. without weather filter; and b. with the weather filter).

open water point has a larger yearly-average value (50.8 K) and smaller variation (2.1 K). The open water tie point has a yearly-averaged value of 38.5 K and 50.8 K before and after filtering the influence of cloud, respectively. The newly-obtained open water point value P_0 becomes larger because of the filtering the influence of clouds and water vapor.

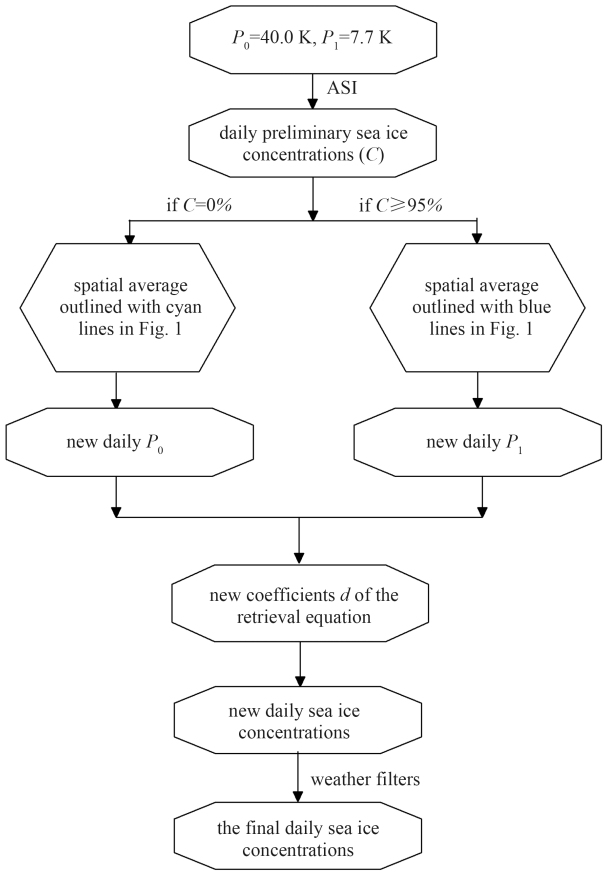

Fig. 2. Flowchart of dynamic tie points sea ice concentration retrieval algorithm.

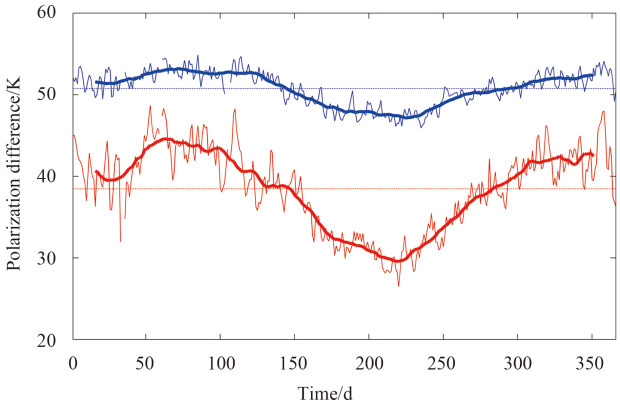

Fig. 3. Comparison of the daily open water tie points before (red) and after (blue) the influence of clouds is filtered for the year 2010 (thin line: daily open water tie points; bold line: 30-d running mean tie points; dashed line: the yearly-averaged tie point).

3.3 *Sea ice concentration based on the dynamic tie points*

By filtering out the influence of clouds, this study produces a dynamic tie points algorithm and obtains the daily tie points by using the data from the year 2010. After obtaining the daily tie points P_0 and P_1, we produce the daily retrieval equation, whose coefficients are determined by the tie points. The open water daily tie points are shown in Fig. 3 and the newly-obtained sea ice tie points are shown in Fig. 4. P_0 is still affected by clouds in the summer, but the effect is smaller compared with that before. P_1 changes little and significantly decreased during the summer, mainly due to the melting of first-year ice in the statistical region circled in Fig. 1 in the summer because the melt ponds developed faster on first-year ice than on multi-year ice (Istomina et al., 2014), making the reduction of first-year ice more obvious. Additionally, the polarization difference for the first-year ice is larger than that of multi-year ice, which makes the obtained sea ice tie points smaller in summer. The yearly-averaged P_0 and P_1 values are 50.8 K and 7.8 K, respectively. Figure 5 compares the results of this study using dynamic tie points, the concentration field of using fixed tie points (Spreen et al., 2008) and the difference between them. The concentration of the former is less than sea ice concentration using fixed tie points in the high-concentration region. The difference mainly occurs in the marginal regions and the inner high-concentration region.

4 Comparison using MODIS data

In previous studies, higher resolution remote sensing data, such as MODIS and AVHRR, were used to compare with the sea ice concentrations obtained from passive microwave remote sensing data. For example, Wiebe et al. (2009) and Ye et al. (2011) obtained the sea ice concentrations from visible light remote sensing data by using a threshold method that counted ice proportions in the corresponding grids based on the ice-water discrimination. While in this paper, the ice concentration retrieved by tie point algorithm from MODIS data (Steffen and Schweiger, 1991, Cavalieri et al., 2010) are used to compare those obtained from the AMSR-E data algorithm. The details will be explained in Section 4.2.

4.1 *The selected regions used for comparison*

Current microwave algorithms tend to underestimate the ice concentration in summer due to the impact of melt ponds (Comiso and Kwok, 1996). The estimation errors are mainly found in the ice edge zone (Cavalieri et al., 2010). Thus, it is necessary to compare the sea ice concentrations from microwave remote

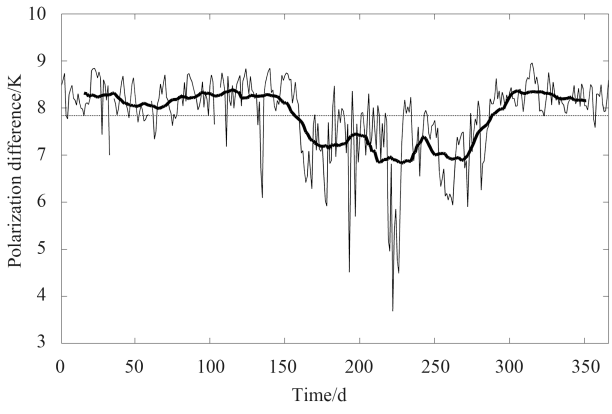

Fig. 4. Daily sea ice tie points of 2010 (illustration is the same as Fig. 3).

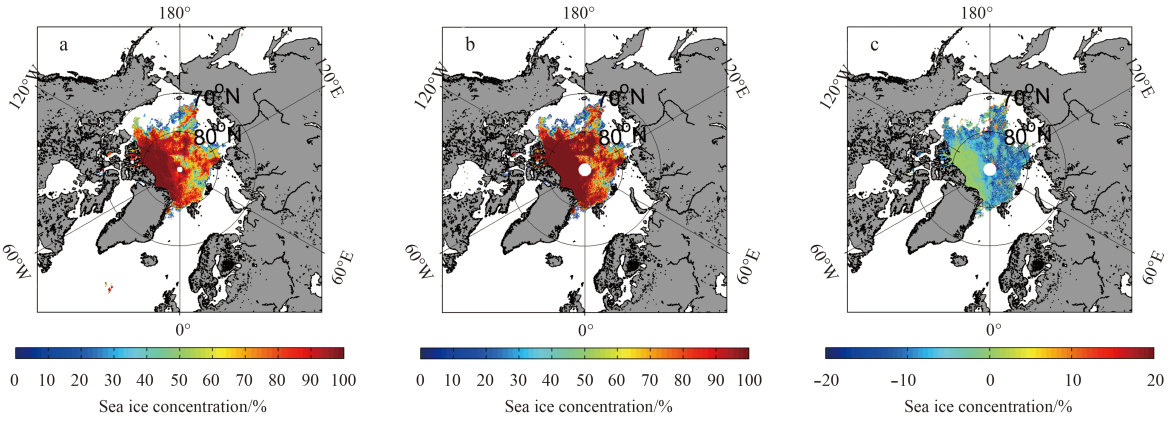

Fig. 5. The Arctic sea ice concentration distributions and differences of the products using fixed tie points and those obtained by dynamic tie points in this study on September 1, 2010 (a. sea ice concentrations obtained by dynamic tie points in this study; b. products by fixed tie points; and c. difference between them.

sensing data, especially in the ice marginal zone, to ensure the reliability of the results. The 12 samples used by Su et al. (2013) for comparison are mainly concentrated in the Bering Sea. Emery et al. (1994) selected 17 AVHRR images mainly located in the Chukchi Sea, and Cavalieri et al. (2006) used 4 cloud-free ETM+ images mainly located in the Bering Sea and the Chukchi Sea to compare with the AMSR-E retrieved products. Here, 40 cloud-free MODIS albedo data (from 21 February to 30 June 2010) are selected to compare with the retrieval results of AMSR-E. It is difficult to select the same size as MODIS sample data because of the impact of clouds. As shown in Fig. 6, the data used for comparison have a longer time range from the freezing to the melting of the ice and wider spatial coverage cover most of the Arctic marginal seas in this study, thus ensuring the comprehensiveness of the comparison.

4.2 *MODIS sea ice concentration*

MODIS Level 1B planetary reflectance (MYD02HKM) was obtained for each of the Bands 1, 3 and 4. A sun-angle correction was applied by dividing the reflectance by the cosine of the sun angle from the MODIS geolocation product (MYD03). And the broadband (0.46–0.67 μm) top-of-the-atmosphere (TOA) albedo was derived from the swath TOA MODIS sun-angle-corrected planetary reflectance in the red (B1), green (B4), and blue (B3) bands using the weights: B1×0.326 5 +B4×0.236 6 +B3×0.436 4 (Liang et al., 1998). Then the broadband TOA albedos were used to calculate MODIS sea ice concentration (Cavalieri et al., 2010) based on the method described in Su et al. (2013). The broadband TOA albedo tie point method is a commonly used method to determine ice or water based on MODIS. In the first step, the sea ice threshold (A_i) and the open water threshold (A_w) are obtained from the broadband TOA albedo data according to Cavalieri et al. (2010). Using the A_w, the ice and water can be discriminated, and for the ice points, the sea ice threshold (A_i) can be obtained by probability statistics, such as a histogram. The A_w we used here is 0.1 for all samples. For different ice thickness and ice type, we use different A_i determined by probability statistics. Based on the sea ice threshold (A_i) and the ice water threshold (A_w), the MODIS 500-m resolution sea ice concentrations can be derived using the traditional tie point algorithm (Steffen and Schweiger, 1991) and broadband TOA albedo data. At last, these results are projected onto the AMSR-E grid.

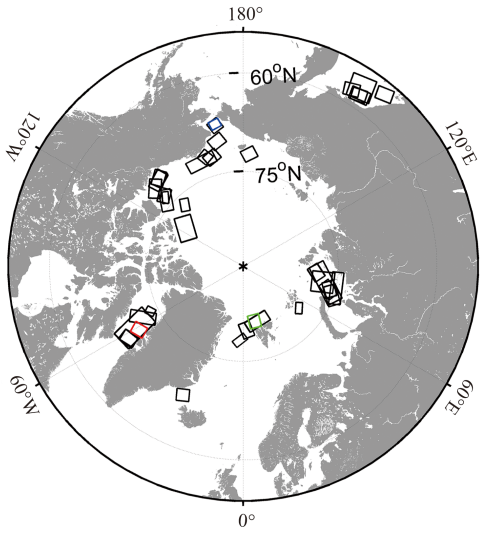

Fig. 6. The locations of the selected MODIS images, the red, green and blue frames are for the locations of samples with numbers of 14, 15 and 34, respectively. Date of the sample is given in Table 2.

Figure 7 shows three examples (Samples 14, 15 and 34) of the 40 samples on April 2, April 3 and May 29, 2010, respectively. They represent (1) the regions with high-concentration ice and narrow leads; (2) the region mixed with high-concentration ice, relatively high concentration and larger leads near ice edges; (3) region of ice edge with lager areas of open water. The locations of these three images are shown in Fig. 6 by the red, green and blue frames. Figure 7 shows MODIS broadband TOA albedo images and sea ice concentration from MODIS data, which suggests that MODIS retrieval algorithm used in this study can clearly portray the actual situation of the Arctic sea ice, especially in sea ice edge region, thus guaranteeing the quality of the data used for comparison.

Figure 8 illustrates the advances in the retrieval results of this study. It shows the sea ice concentrations retrieved using dynamic ASI algorithm with daily changed tie points (red line) and the original ASI algorithm with fixed tie points (black line, P_0=47.0 K and P_1=11.7 K) for different polarization difference values in three dates (April 2, April 3, and May 29), respectively. The water

and sea ice tie points of three sets used by the dynamic tie points algorithm to produce Fig. 8 are (53.5 K, 8.0 K), (51.9 K, 8.2 K) and (49.6 K, 8.7 K), respectively. All the three canvases show that in the higher (lower) sea ice concentration region, the values retrieved by the dynamic tie point ASI algorithm are smaller (larger) than those retrieved by fixed tie point ASI algorithm. Figure 8 shows a decrease (increase) the sea ice concentration in the higher (lower) sea ice concentration region compared with the ASI algorithm. According to Wiebe et al. (2009), the ASI algorithm had underestimated sea ice concentrations at the ice edges and overestimated them in the inner region of ocean. Therefore, the dynamic tie points ASI algorithm modifies the retrieval in the right direction. However, it remains to be investigated to which extent the weaknesses of the original ASI algorithm are corrected.

4.3 *The result of comparison*

The retrieval results of the three samples mentioned above are compared with sea ice concentration products by using fixed tie points in Fig. 9. It can be seen that the sea ice concentrations retrieved using dynamic tie point ASI algorithm are smaller than those obtained using fixed tie point algorithm as a whole. For Sample 14, the MODIS sea ice concentration can depict the narrow leads, while those derived from AMSR-E cannot well show them. And the sea ice concentration using dynamic tie points reduce the ice concentration in high ice concentration region compare with those from using fixed tie points. For Sample 15, all the sea ice concentration can depict the large leads, but the MODIS result is more detailed. And in the inner ice pack, the ice concentration of this study are closer the MODIS result within the ice edge with a relatively lower value compare with the products from the fixed tie point, while in the position of ice edge line the concentration is larger than those from the fixed tie points. For Sample 34, the sea concentration using dynamic tie points are larger and closer to the ice edge than that using fixed tie points. Compared with the MODIS results (see Panels a and d in Fig. 9), both of the dynamic and fixed tie points results for Samples 14, 15 and 34 are larger than the MODIS results, it is difficult for AMSR-E remote sensing data to discriminate ice and water in detail due to poor resolution of the AMSR-E grids. However, the results using dynamic tie points are closer to the MODIS results.

The positions of the ice edge lines are shown in Panels a and d of Fig. 9 for Samples 15 and 34. For Sample 15, the ice edges line are almost in the same position, retrieved by using two algorithms of dynamic and fixed tie points, and both coincide with the MODIS based ice edge. For Sample 34, both the microwave based ice edges are shifted by few pixels toward open water compared with the MODIS results. The disagreement occurred when there are lots of scattered ice floes in the region where ice nearly free according MODIS. But on the scale of AMSR-E 89 GHz these

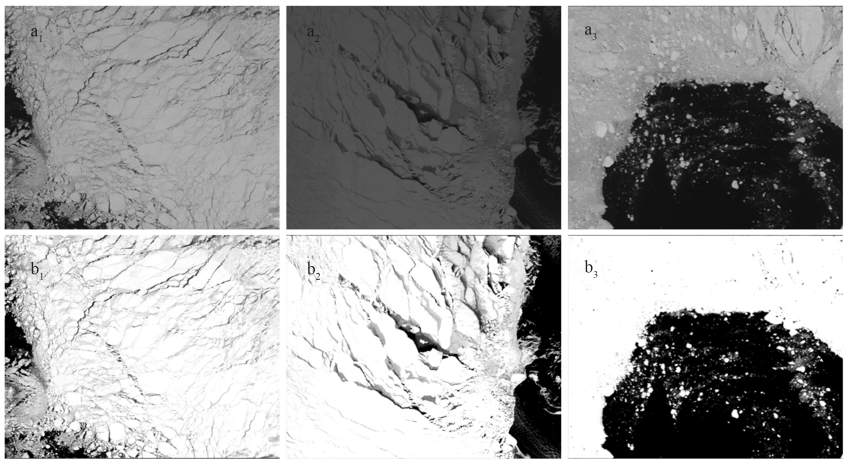

Fig. 7. MODIS broadband TOA albedo images and sea ice concentrations calculated by tie point algorithm in row (a) and row (b), respectively. (left column: Sample 14; middle column: Sample 15; right column: Sample 34).

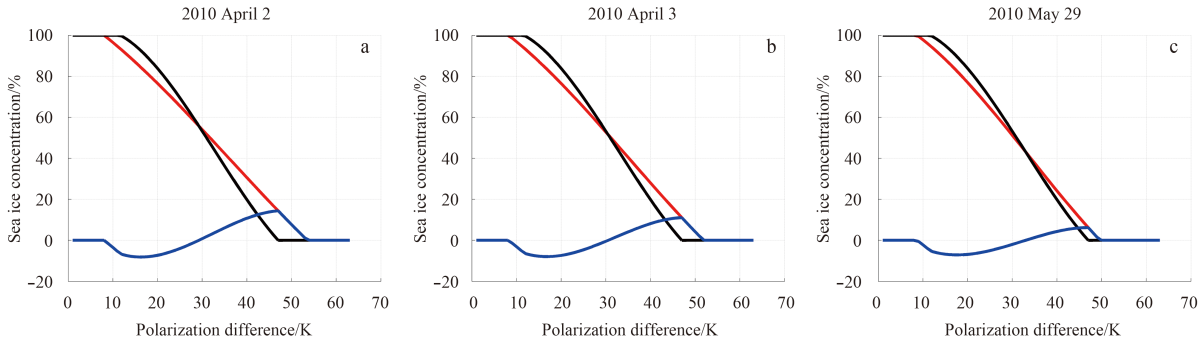

Fig. 8. Comparison between the sea ice concentrations retrieved by dynamic tie point ASI algorithm (red line) and those using fixed tie point algorithm (black line) from AMSR-E data. Here blue line denotes the difference of sea ice concentrations retrieved by two different equations; the horizontal ordinate denotes the different polarization difference values of AMSR-E data.

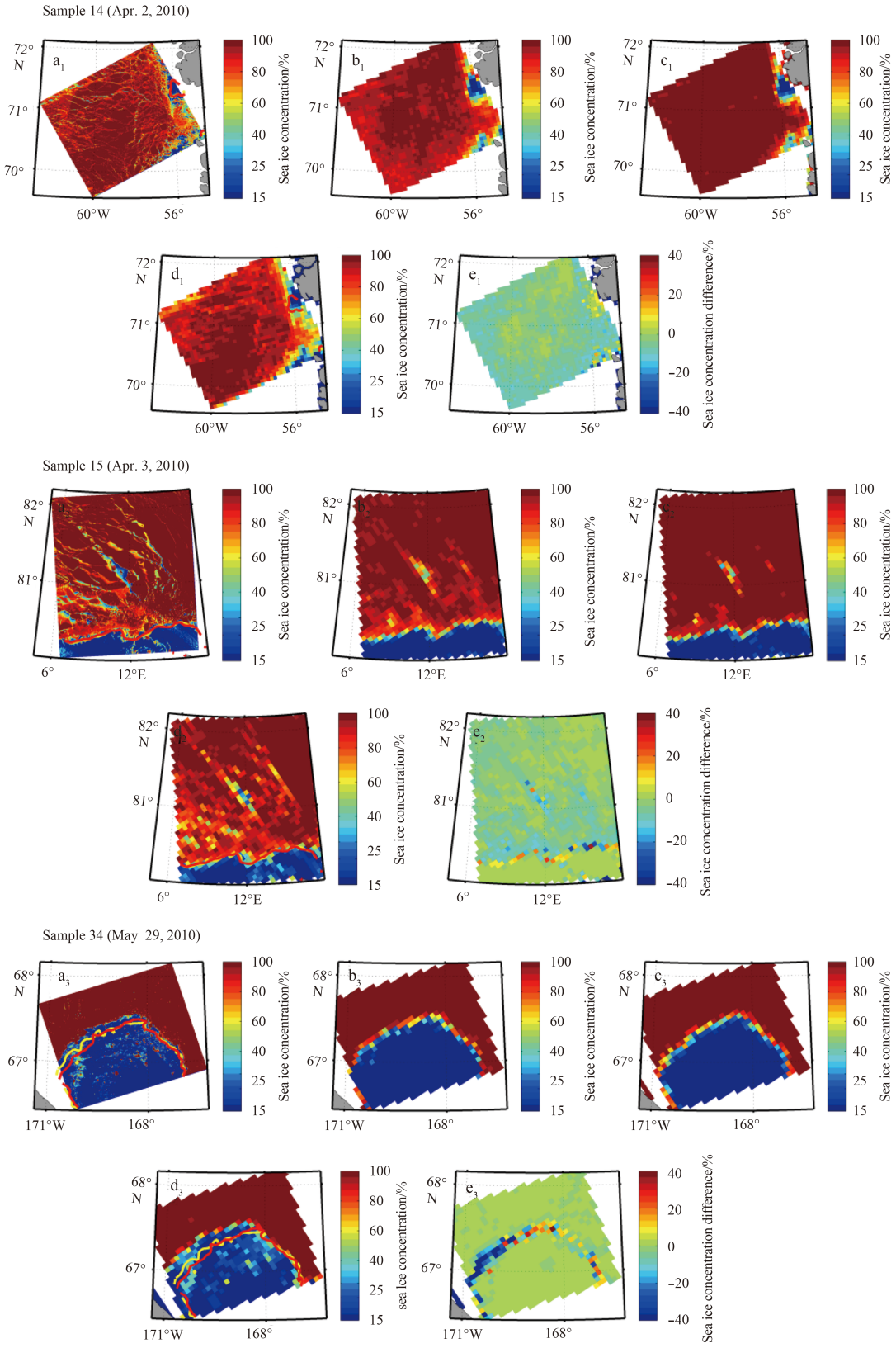

Fig. 9. The sea ice concentration (%) for the three selected samples. a. 500-m resolution sea ice concentrations calculated using MODIS data; b. sea ice concentration using dynamic tie points; c. sea ice concentration product using fixed tie points; d. sea ice concentration projected on 6.25 km grid calculated using MODIS data; and e. the difference between sea ice concentration using dynamic tie points and products using fixed tie points. The yellow line on the MODIS map represents the sea ice concentration contour 15% based on the results using dynamic of this study, the red line represents the 15% contour of sea ice concentrations using fixed tie points for Sample 15, and 34.

few flows are still enough to cause an ASI ice concentration greater than 15%. However, the ice edges obtained using dynamic tie points (yellow line) are a little closer to those obtained using MODIS data, compared with those obtained using fixed tie point (red line).

The spatially averaged sea ice concentrations for the 40 selected regions are calculated for each sample by using fixed tie points and dynamic tie points. Figure 10 shows these two results, as well as the spatially averaged sea ice concentrations calculated using MODIS data. In Fig. 10, the samples are ordered by time from February to June (Table 2). It shows that the rough trend of sea ice concentrations is to decline. Though the time changed from winter to summer, the selected samples are from different regions; therefore, the results shown in Fig. 10 do not always follow the seasonal variability. In most case, the spatial average ice concentrations by using dynamic tie points are closer to the MODIS results than those by using fixed tie points.

The mean differences and the root mean square (RMS) differences between the sea ice concentrations retrieved from 40 selec-

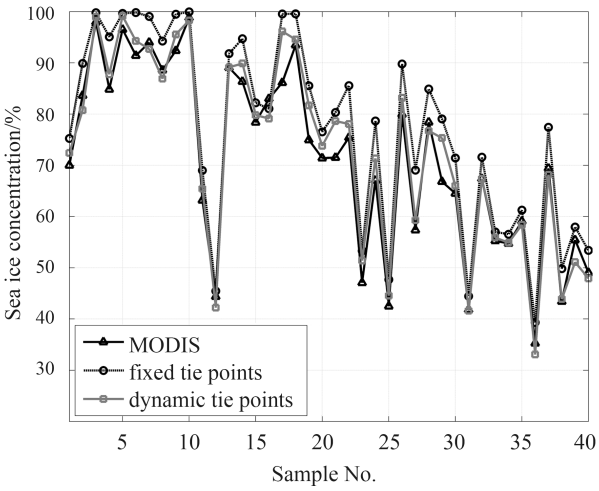

Fig. 10. The average sea ice concentrations of the 40 selected samples. Date of the sample numbers see Table 2.

Table 2. Statistical errors of AMSR-E sea ice concentrations and MODIS results[1)] (ASI-MODIS, %)

Sample index	Date	Fixed tie points MD (P_0=47 K, P_1=11.7 K)	Dynamic tie points MD (daily P_0 and P_1)	Fixed tie points RMS difference (P_0=47 K, P_1=11.7 K)	Dynamic tie points RMS difference (daily P_0 and P_1)
1	Feb. 21	5.24	2.41	21.96	22.87
2	Feb. 26	6.28	–2.85	14.02	13.75
3	Mar. 01	1.86	1.03	8.47	8.17
4	Mar. 02	10.14	2.95	13.98	11.13
5	Mar. 02	3.12	2.61	9.39	9.35
6	Mar. 03	8.41	2.86	13.01	10.79
7	Mar. 06	5.09	–1.28	12.26	11.57
8	Mar. 09	5.66	–1.68	11.82	10.38
9	Mar. 10	7.12	3.17	11.46	9.95
10	Mar. 14	1.18	–0.50	5.97	6.13
11	Mar. 22	5.82	2.25	13.86	11.75
12	Mar. 22	1.10	–2.13	25.11	22.91
13	Mar. 26	2.77	0.08	15.20	14.70
14	**Apr. 02**	**8.38**	**3.54**	**13.88**	**11.10**
15	**Apr. 03**	**3.82**	**1.44**	**13.73**	**12.12**
16	Apr. 03	–1.94	–3.85	10.07	10.10
17	Apr. 08	13.42	10.00	17.37	15.14
18	Apr. 08	6.12	1.10	10.32	8.79
19	Apr. 12	10.57	6.73	15.69	17.43
20	Apr. 16	5.12	2.37	13.38	19.22
21	Apr. 17	8.83	7.14	15.74	17.84
22	Apr. 25	10.16	2.66	16.99	13.15
23	Apr. 25	6.23	4.34	11.86	12.81
24	Apr. 25	11.59	4.29	16.16	11.07
25	May 02	5.21	2.09	18.88	16.55
26	May 03	9.86	3.24	14.33	10.54
27	May 14	11.70	1.94	19.28	13.61
28	May 24	6.48	–1.70	15.58	14.12
29	May 26	12.26	8.52	17.52	15.08
30	May 27	6.91	1.52	15.99	13.53
31	May 28	2.66	–0.19	19.16	18.79
32	May 28	4.23	0.00	16.20	17.91
33	May 28	1.75	0.66	9.57	11.18
34	**May 29**	**1.81**	**0.15**	**20.51**	**18.19**
35	Jun. 04	2.02	–0.67	15.33	15.46
36	Jun. 21	4.06	–2.19	11.20	8.70
37	Jun. 21	8.00	–1.25	12.57	8.88
38	Jun. 22	6.43	0.49	11.49	8.84
39	Jun. 30	2.55	–4.31	17.17	16.36
40	Jun. 30	4.36	–1.11	18.65	16.69
Mean		5.91	1.40	14.63	13.42

Notes: [1)] mean difference; RMS difference: root mean square difference.

ted MODIS samples and those retrieved from AMSR-E data using fixed tie points and dynamic tie points are calculated and are summarized in Table 2. As shown in Table 2, the mean differences between the two AMSR-E retrieval sea ice concentrations and the MODIS sea ice concentrations are 5.91% for the products using fixed tie points and 1.40% for sea concentrations using dynamic tie points, respectively. The RMS differences of them are 14.63% and 13.42% respectively. In all of 40 samples, 95% and 75% of sea concentrations obtained using dynamic tie points have smaller mean differences and the RMS differences than those obtained using fixed tie points separately compared with the MODIS results.

In terms of the mean differences, the sea ice concentrations of AMSR-E results are larger than those of MODIS for most of the samples. This primarily due to where at the lowest polarization differences the retrieved ice concentration is constantly 100% so that small variations in the polarization differences, as caused by a small fraction of open water, in a footprint otherwise covered by ice will not be reflected in the retrieved ice concentration for AMSR-E data. The mean differences for products using fixed tie points are positive except Sample 16, while those obtained using dynamic tie points, there are 32.5% of the 40 samples are negative. Among the 40 samples, only one (Sample 17) has the mean difference larger than 10% for the sea ice concentrations obtained using dynamic tie point ASI algorithm.

The sea ice concentrations with the RMS differences larger than 15% are found in 19 of 40 samples when fixed tie point ASI algorithm is used, and 14 of 40 samples when dynamic tie point ASI algorithm is used. For the samples with RMS differences are greater than 15%, there are mainly two reasons: (1) The leads in high ice concentration region can clearly observed by MODIS, rather than AMSR-E data, which lead to larger RMS differences; (2) in the marginal ice zone, there are more mixed ice and water regions, MODIS sensor with higher spatial resolution can discriminate ice and water sufficiently while the AMSR-E data cannot. Overall, the mean differences and RMS differences of sea ice concentration using dynamic tie points are smaller than the products using fixed tie points.

5 Conclusions and discussion

Spreen et al. (2008) and Su et al. (2013)'s studies indicated the determination of tie points in ASI algorithm is important to the accuracy of retrieved sea ice concentrations. In this paper, we performed tests to develop ASI algorithm using dynamic tie points. Based on the sea ice concentrations retrieved from Aqua MODIS with clear atmosphere condition, the sea ice concentrations retrieved from AMSR-E data using dynamic tie point ASI algorithm and ASI algorithm with fixed tie points are compared to each other. By comparing with the retrieval equations with the dynamic and fixed tie points, it is found that the dynamic tie point algorithm can improve the accuracy of sea ice concentrations retrieved from AMSR-E data to some extent. Also, the ice concentration results from this study have a smaller difference from MODIS results than those from the products using fixed tie point. The main conclusions are as follows:

(1) Base on dynamic algorithms suitable to SSMI/SMMR data (Eastwood et al., 2011), a dynamic tie points ASI algorithm has been achieved in this paper. Daily tie points can be obtained using this algorithm, and the average sea ice tie point (P_1) in 2010 was 7.8 K. This value is smaller than 10.0 K of Su et al. (2013), which was estimated with fixed regional statistics. The sea ice tie point is determined based on initially-estimated ice concentrations greater than 95%. It's worth to mention that, in the calculating the open water tie points (P_0), we exclude the impact of clouds and water vapor, which otherwise may introduce erroneous ice concentration estimates. The average open water tie point was 50.8 K for the 2010 data and was also greater than that from fixed regional statistics (46.7 K). Additionally, the amplitudes of variation in open water and sea ice tie points were both smaller than that of the fixed regional statistics. As a result of smaller ice tie point and larger water tie point, the retrieved sea ice concentrations increased in low concentration areas and decreased in high concentration areas, respectively. This reduced the ice concentration retrieval errors from microwave data to some extent, which corresponds with the results shown in Fig. 8.

(2) The MODIS retrieved results can obtain information of open water leads in high ice concentration areas and ice edges regions. 40 cloud-free MODIS images were selected to retrieval ice concentration calculated by tie point algorithm and were used to compare with the concentrations retrieved from AMSR-E data. Compared with the sea ice concentrations retrieved from MODIS data, the mean difference of products using fixed tie points and the results of this study were 5.91% and 1.40%, respectively, and their RMS differences were 14.63% and 13.42%, respectively. Relative to the MODIS results, 95% of 40 samples had lower mean differences and 75% of samples had lower RMS differences than those of products by fixed tie points.

The dynamic tie points ASI algorithm has successfully excluded the effects of clouds in the determination of the open water tie point. However, it is still difficult to remove the cloud impact on the determination of ice tie points. The daily sea ice tie points fluctuation is mainly caused by the variety of the physical temperature of the ice, but the cloud effect also contributes to the fluctuation as well. Therefore, further effort is necessary to get rid of the weather influence. Taking into account the effect of daily tie point value variation in the retrieval results, we also used 30-d running mean tie points to derive sea ice concentrations (not show in this study) and compared the results with MODIS sea ice concentrations. The mean differences and RMS differences were 1.25% and 13.36%, respectively, which are not significantly different from those using daily tie points. As the MODIS data are taken during March to June because of the cloud, further comparison by higher resolution data during summer is needed in future. Besides, at present, the errors of ice category are far more than the retrieval of sea ice concentration. If ice classification algorithms will be good enough, the ice category-dependent daily tie points will also be worth to be studied. This dynamic tie points ASI algorithm can also be used with AMSR2 data and can achieve longer time series of 6.25 km resolution sea ice concentration products, from which the analysis of sea ice variability in polar region will benefit.

Acknowledgement

We thank Spreen Gunnar, Cheng Bin, Heygster Georg, Hu Xianmin and Li Xiang reading the manuscript and providing useful comments that improved the paper. We also give our thanks to Liu Yuguang for the English smoothing.

References

Bi Haibo, Huang Haijun, Su Qiao, et al. 2014. An Arctic sea ice thickness variability revealed from satellite altimetric measurements. Acta Oceanologica Sinica, 33(11): 134–140

Cavalieri D J, Gloersen P, Campbell W J. 1984. Determination of sea ice parameters with the Nimbus 7 SMMR. Journal of Geophysical Research, 89(D4): 5355–5369

Cavalieri D J, St Germain K M. 1995. Arctic sea ice research with satellite passive microwave radiometers. IEEE Geoscience and Remote Sensing Society Newsletter, 97(1): 6–12

Cavalieri D J, Markus T, Hall D K, et al. 2006. Assessment of EOS-AQUAAMSR-EArctic sea ice concentrations using landsat-7 and airborne microwave imagery. IEEE Transactions on Geoscience and Remote Sensing, 44(11): 3057–3069

Cavalieri D J, Markus T, Hall D K, et al. 2010. Assessment of AMSR-E Antarctic winter sea-ice concentrations using Aqua MODIS. IEEE Transactions on Geoscience and Remote Sensing, 48(9): 3331–3339

Comiso J C. 1995. SSM/I sea ice concentrations using the bootstrap algorithm. National Aeronautics and Space Administration. NASA RefPubl, RP 1380, 49

Comiso J C, Kwok R. 1996. Surface and radiative characteristics of the summer Arctic sea ice cover from multisensor satellite observations. Journal of Geophysical Research, 101(C12): 28397–28416

Comiso J C, Cavalieri D J, Markus T. 2003. Sea ice concentration, ice temperature, and snow depth using AMSR-E data. IEEE Transactions on Geoscience and Remote Sensing, 41(2): 243–252

de Vernal A, Gersonde R, Goosse H, et al. 2013. Sea ice in the paleoclimate system: the challenge of reconstructing sea ice from proxies—an introduction. Quaternary Science Reviews, 79: 1–8

Eastwood S, Larsen K R, Lavergne T, et al. 2011. Global Sea Ice Concentration Reprocessing Product User Manual, Version 1.3, EUMETSAT

Emery W J, Fowler C, Maslanik J. 1994. Arctic sea ice concentrations from special sensor microwave imager and advanced very high resolution radiometer satellite data. Journal of Geophysical Research, 99(C9): 18329–18342

Gloersen P, Cavalieri D J. 1986. Reduction of weather effects in the calculation of sea ice concentration from microwave radiances. Journal of Geophysical Research, 91(C3): 3913–3919

Han H, Lee H. 2007. Compartive study of sea ice concentration by using DMSP SSM/I, Aqua AMSR-E and Kompsat-1 EOC. In: IEEE InternationalGeoscience and Remote Sensing Symposium, 2007. IGARSS 2007. Barcelona, Spain: IEEE, 4249–4252

Kaleschke L, Lüpkes C, Vihma T, et al. 2001. SSM/I sea ice remote sensing for mesoscale ocean-atmosphere interaction analysis: Ice and icebergs. Canadian Journal of Remote Sensing, 27(5): 526–537

Kern S. 2001. A new algorithm to retrieve the sea ice concentration using weather-corrected 85GHz SSM/I measurements. Logos-Verlag, Institute of Environmental Physics, Bremen, Germany

Kern S, Heygster G. 2001. Sea-ice concentration retrieval in the Antarctic based on the SSM/I 85. 5 GHz polarization. Annals of Glaciology, 33(1): 109–114

KernS, Kaleschke L, Clausi D A. 2003. A comparison of two 85-GHz SSM/I ice concentration algorithms with AVHRR and ERS-2 SAR imagery. IEEE Transactions on Geoscience and Remote Sensing, 41(10): 2294–2306

Kern S. 2004. A new method for medium-resolution sea ice analysis using weather-influence corrected Special Sensor Microwave/Imager 85 GHz data. International Journal of Remote Sensing, 25(21): 4555–4582

Liang Shunlin, Strahler A, Walthall C. 1998. Retrieval of land surface Albedo from satellite observations: A simulation study. In:IEEE International Geoscience and Remote Sensing Symposium Proceedings. Seattle, WA: IEEE, 1286–1288

Liu Jiping, Curry J A, Martinson D G. 2004. Interpretation of recent Antarctic sea ice variability. Geophysical Research Letters, 31(2)

Markus T, Cavalieri D J. 2000. An enhancement of the NASA Team sea ice algorithm. IEEE Transactions on Geoscience and Remote Sensing, 38(3): 1387–1398

Meier W N. 2005. Comparison of passive microwave ice concentration algorithm retrievals with AVHRR imagery in Arctic peripheral seas. IEEE Transactions on Geoscience and Remote Sensing, 43(6): 1324–1337

Rind D, Healy R, ParkinsonC, et al. 1995. The role of seaice in $2\times CO_2$ climate model sensitivity. Part I: The total influence of sea ice thickness and extent. Journal of Climate, 8(3): 449–463

Serreze M C, Maslanik J A, Scambos T A, et al. 2003. A record minimum arctic sea ice extent and area in 2002. Geophysical Research Letters, 30(3): 1110

Spreen G. 2004. Meereisfernerkundung Mit Dem Satellitengestützten Mikrowellenradiometer AMSR (-E)—Bestimmung der Eiskonzentration und Eiskante unter Verwendung-der-89-GHz-Kanäle, Diplomarbeit [dissertation] (in German). Hamburg, Germany: Universityof Hamburg

Spreen G, Kaleschke L, Heygster G. 2008. Sea ice remote sensing using AMSR-E 89-GHz channels. Journal of Geophysical Research, 113(C2)

Steffen K, Schweiger A. 1991. NASA team algorithm for sea ice concentration retrieval from Defense Meteorological Satellite Program special sensor microwave imager: Comparison with Landsat satellite imagery. Journal of Geophysical Research, 96(C12): 21971–21987

Svendsen E, Matzler C, Grenfell T C. 1987. A model for retrieving total sea ice concentration from a spaceborne dual-polarized passive microwave instrument operating near 90 GHz. International Journal of Remote Sensing, 8(10): 1479–1487

Su Jie, Hao Guanghua, Ye Xinxin, et al. 2013. The experiment and validation of sea ice concentration AMSR-E retrieval algorithm in polar region. Journal of Remote Sensing (in Chinese), 173(3): 495–513

Vavrus S, Harrison S P.2003. The impact of sea-ice dynamics on the Arctic climate system. Climate Dynamics, 20(7–8): 741–757

Wiebe H, Heygster G, Markus T.2009. Comparison of the ASI ice concentration algorithm with Landsat-7 ETM+ and SAR imagery. IEEE Transactions on Geoscience and Remote Sensing, 47(9): 3008–3015

Ye Xinxin, Su Jie, Wang Yang, et al. 2011.Assessment of AMSR-E sea ice concentration in ice margin zone using MODIS data. In: 2011 International Conference onRemote Sensing, Environment and Transportation Engineering (RSETE). Nanjing, China: IEEE, 3869–3873

Zhang S G. 2012. Sea ice concentration algorithm and study on the physical process about sea ice and melt-pond change in central Arctic [dissertation]. Qingdao, China: Ocean University of China

Zhang Shugang, Zhao Jinping, Frey K, et al. 2013. Dual-polarized ratio algorithm for retrieving Arctic sea ice concentration from passive microwave brightness temperature. Journal of Oceanography, 69(2): 215–227